Available online at www.sciencedirect.com
ScienceDirect
International Journal of Engineering Science 44 (2006) 927–937
International Journal of Engineering Science
www.elsevier.com/locate/ijengsci

Effect of surface roughness on gas flow in microchannels by molecular dynamics simulation

Bing-Yang Cao *, Min Chen, Zeng-Yuan Guo

Department of Engineering Mechanics, Tsinghua University, Beijing 100084, People's Republic of China

Received 4 February 2006; received in revised form 15 June 2006; accepted 15 June 2006

Abstract

Understanding the effect of surface roughness on gas flow in microchannels is highly desirable in microfluidic devices. Non-equilibrium molecular dynamics simulation is applied to investigate the effect of the surface roughness on slip flow of gaseous argon in submicron platinum channels. The geometries of the surface roughness are modeled by triangular, rectangular, sinusoidal and randomly triangular waves respectively. The results show that the boundary conditions of velocity slip, including slip, no-slip and negative slip, depend not only on the Knudsen number but also on the surface roughness. Induced by the roughness, the slip length of gas microflow over a rough surface is less than that predicted by the Maxwell model and shows a non-linear relationship with the Knudsen number. The friction coefficient increases not only with decreasing the Knudsen number but also with increasing the surface roughness. The impacts of the surface roughness and the gas rarefaction on the friction coefficient of gas microflow are strongly coupled. The roughness geometry also shows significant effects on the boundary conditions and the friction characteristics. The distortion of the streamlines and the enhancement of the penetrability near the rough surface are demonstrated to be responsible for the roughness effect.

Keywords: Microscale flow; Rarefaction effect; Surface roughness; Velocity slip; Molecular dynamics

1. Introduction

Due to the rapid advancement of micromachining technology over the past decades, it has been feasible to fabricate micro- and nano-devices known as MEMS and NEMS (micro/nano-electro-mechanical systems) [1,2]. Flow physics on the microscale has attracted considerable attention recently [3,4]. A number of literatures show that flows on the microscale are quite different from those on the macroscale [3–6]. For flows on the macroscale, the effect of surface roughness on the flow friction is often characterized by the Moody chart, in which the friction factor is independent of the surface roughness for laminar flows with a relative roughness less than 5% [7]. However, in microscale flow systems, as the relative roughness becomes very large,

* Corresponding author. Tel./fax: +86 10 62781610.
E-mail address: caoby@tsinghua.edu.cn (B.-Y. Cao).

0020-7225/$ - see front matter © 2006 Elsevier Ltd. All rights reserved.
doi:10.1016/j.ijengsci.2006.06.005

the roughness effect cannot be ignored [8,9]. Especially, for gas flow in microchannels, if the Knudsen number (Kn) is in the range of 0.001–0.1, the flow falls in the slip regime and the rarefaction effect appears in the region adjacent to the channel surface about a mean free path (MFP) of gas molecules. Up until now, most of the theoretical, analytical and numerical approaches concerning the rarefaction of gas microflows are still limited to mathematically smooth surfaces where the surface roughness is assumed to be much smaller than the MFP [10]. In practical microengineering situations, the surface roughness in micro-fabricated channels may often be comparable to the MFP [11,12]. The surface roughness may play a remarkable role in momentum transport of the gas microflow.

In recent years, some literatures [13–17] on the study of rarefied gas flow in microchannels with surface roughness have been published. Turner et al. [13] experimentally measured the friction coefficient of slip flows of air and helium in microchannels and observed that the surface roughness might cause a larger friction than the theoretical prediction. However, the deviation of the flow frictions for the smooth and rough channels was within the large experimental uncertainty. Thus, the promising solution points to numerical methods. Using Monte Carlo (MC) method, Sugiyama et al. [14] investigated the free-molecule and near-free-molecule flow conductance through microchannels with roughness modeled by conical units and a decrease of the channel conductance induced by the roughness was observed. Focusing on the slip and transition flow, Sun and Faghri [15] performed a direct simulation Monte Carlo (DSMC) study, in which the roughness was modeled by an array of rectangular modules, and found that the friction coefficient increased with increasing roughness height and decreasing distance between the roughness modules. Unfortunately, it is very difficult for the MC method to consider potential interactions between particles and more complicated boundary conditions. Based on molecular dynamics (MD) simulations, Mo and Rosenberger [16] obtained velocity profiles of fluid flow in two-dimensional (2D) microchannels roughened sinusoidally and randomly. It was found that the no-slip boundary condition (BC) was a consequence of the commensuration of the MFP and the surface roughness. Cao et al. [17] showed the characteristics of boundary conditions and flow friction of gas microflows affected by the surface roughness modeled by triangular unit arrays using the MD method. Also, some phenomenon models were proposed to predict the roughness effect on microflows, for example, the viscosity model by Mala and Li [18], the porous media model by Tichy [19] and the Brinkman-extended Darcy model by Li et al. [20]. However, the mechanism and law of the roughness effect on gas microflows has yet been lack of clarification from the molecular scale point of view.

For the purpose of clarifying the effect of the surface roughness on rarefied gas flow in microchannels, we carry out non-equilibrium molecular dynamics (NEMD) simulations to investigate locally fully developed (LFD) flows of gaseous argon in submicron platinum channels, whose walls are roughened by surface structures of triangular, rectangular, sinusoidal and randomly triangular waves. Velocity profiles, boundary conditions, friction coefficient and flow fields near rough surfaces affected by the surface roughness and the rarefaction are presented in this paper.

2. Simulation details

Our molecular dynamics simulations consider a 2D system of N argon molecules enclosed between two parallel platinum walls as shown in Fig. 1(a). The Poiseuille flow is induced by subjecting the gas molecules to an external driving field $g_x = 3.7 \times 10^{10}\ \mathrm{m/s^2}$. The flow is locally fully developed to be laminar with Reynolds numbers in the range of 5–50. Due to the high computation efficiency of the two-dimensional molecular dynamics (2DMD) method [21], the simulated characteristic length, i.e. the distance separated between the two plates, reaches $H = 0.10\ \mu\mathrm{m}$ ($h = H/2$) which is really comparable with the characteristic size of MEMS/NEMS devices in engineering situations. In the x direction, the size of the simulation cell is about $L = 0.1\ \mu\mathrm{m}$ which is also determined by the roughness geometry in an individual computation. A periodic boundary condition is imposed along the x direction.

Besides the smooth wall, four types of solid walls are roughened in our simulations as shown in Fig. 1(b). The first three types of walls are with periodic structures including (i) rectangular, (ii) sinusoidal and (iii) triangular waves. They can be characterized by the roughness amplitude A and the period P. The roughness periodicity parameter is defined as $p = P/A$. $p = 2.31$ is adopted in all our MD runs. The forth geometry of the surface roughness is (iv) the randomly triangular wave that follows a self-affine fractal statistics approxi-

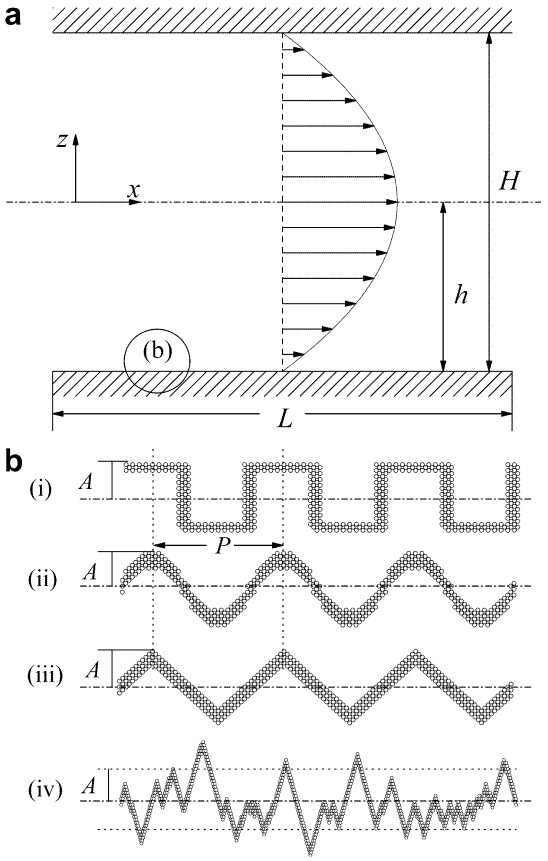

Fig. 1. Schematic diagram of the simulation system. (a) The 2D Poiseuille flow system; (b) four roughness geometries: (i) rectangular, (ii) sinusoidal, (iii) triangular and (iv) randomly triangular wave.

mately. In the literatures, the roughness of a micro-machined surface was found to be able to be described as fractal structures [22] and it could also be characterized by a Gaussian shape of the height distribution [23]. In our simulations, we build the self-affine shape by employing a series of consecutive triangular modules. The height of the modules is selected from the Gauss function

$$f(R) = \frac{1}{\sqrt{2\pi A}} \exp\left(-\frac{R}{2A}\right), \tag{1}$$

where R is the module height and A represents the root-mean-square (RMS) size of the roughness. In course of building the walls by placing atoms onto their lattice sites, we set local roughness within a module through creating smaller modules in a certain probability. In our operations, the probability is taken to be 10%. The fractal dimension is about 1.2, which agrees with the experimentally measured roughness well [22]. In the present paper, the roughness heights are set to be a series of sizes of 0.6–4.8 nm with an internal of 0.6 nm.

For gas–gas and gas–solid interactions between particles, the Lennard-Jones (LJ) potential is applied in the form

$$\phi(r) = 4\varepsilon\left[\left(\frac{\sigma}{r}\right)^{12} - \left(\frac{\sigma}{r}\right)^{6}\right], \tag{2}$$

where r is the intermolecular distance, ε and σ are the energy and diameter parameters respectively. For argon–argon interaction, $\sigma = 3.405 \times 10^{-10}$ m is chosen as a length unit and $\varepsilon = 1.67 \times 10^{-21}$ J is applied as an energy unit. We use $\sigma_{gs} = 3.085 \times 10^{-10}$ m and $\varepsilon_{gs} = 0.894 \times 10^{-21}$ J for argon–platinum interaction [24]. On the basis of Einstein theory, the wall atoms vibrate around their lattice sites, which form a face-centered-cubic (FCC)

plane with a lattice constant $c = 2.776 \times 10^{-10}$ m, attached by springs. The spring stiffness k is controlled by the Einstein temperature

$$k = \frac{16\pi^4 k_B^2 m^2 \theta}{h^2}, \tag{3}$$

in which $k_B = 1.38 \times 10^{-23}$ J/K and $h = 6.63 \times 10^{-34}$ J s is the Boltzmann and Plank constants respectively, $m = 32.4 \times 10^{-26}$ kg is the mass of a wall atom and the Einstein temperature is $\theta = 180$ K. The stiffness is also examined to meet the Lindemann criterion [25].

The equations of particle motion are integrated by the Leapfrog-Verlet algorithm with a MD time step $\tau = 2.146$ ps [26]. The LJ potential is typically truncated and shifted at $r_{cut} = 2.5\sigma$. The gas and wall temperatures are both fixed at $T = 119.8$ K. The velocity rescaling technique is applied to wall atoms to maintain a constant wall temperature. The fluid system is kept at a constant temperature by a Langevin thermostat method in the z direction. The motion equation of the ith molecule is

$$m\ddot{z}_i = \sum_{j \neq i} \frac{\partial \phi_{LJ}}{\partial z_i} - m\Gamma \dot{z}_i + \eta_i, \tag{4}$$

where Γ is a friction constant determining the rate of heat exchange between the simulation system and the heat reservoir, and η_i is a Gaussian distributed random force [27]. A typical computation in our simulations requires 1,000,000 time steps to reach a steady flow state. We spend about 3,000,000 additional time steps on averaging the macroscopic characteristics.

3. Results and discussion

3.1. Velocity profile

The velocity profile can often present us the most elementary information for understanding the microflow characteristics. However, it has nearly not been feasible for the existing visualization technique to observe the velocity profile of gas microflow thus far. In the case of the planar Poiseuille flow of a Newtonian fluid under constant external force, the macroscopic hydrodynamics gives a parabolic solution of the Navier–Stokes (NS) equation. Considering the slip boundary condition, the velocity profile of a LFD laminar flow may be written as

$$u_x = \frac{\rho g_x}{2\mu}(h^2 - z^2) + u_s, \tag{5}$$

in which z is the distance from the middle of the channel, ρ is the density of gases, μ is the dynamical viscosity and u_s is the slip velocity at the gas–solid boundary.

In our simulations, in order to observe the velocity profile across the microchannels, we divide the whole channel into many narrow bins to run averages of their macroscopic velocity. The segmental width of each bin is about $\Delta z = 3.405$ nm (10σ). The velocity profiles in x direction obtained by our simulations are shown in Fig. 2. The velocities have been scaled with the maximum velocity u_m, i.e. the velocity along the microchannel centerline. The positions of $z/H = -0.5$ and 0.5 mean the gas–solid boundaries for the smooth walls or the centerlines of the roughness geometries. Though the local velocities of the gases at the gas-wall boundary are either non-zero or zero depending on the rarefaction and roughness effect, all the velocity profile curves appear quadratic well in the middle of the microchannels. These are actually the cases predicted by Eq. (5). It indicates that the mainstream regime of the gas slip flows in the rough microchannels obeys the continuum mechanics characterized by the NS equation. Thus, it also provides us a foundation for the following quantitative analyses.

The rarefaction effect on the velocity profiles of the gas flows in the smooth microchannels is illustrated in Fig. 2(a). The velocities at the walls are non-zero for the Knudsen number in the range of 0.01–0.15, which is often defined as a velocity slip. For $Kn = 0.04$, the slip velocity is $u_s = 0.4\sigma/\tau$, and for $Kn = 0.10$, $u_s = 0.5\sigma/\tau$. A larger Knudsen number always brings on a larger velocity slip, which is the consequence of the non-equilibrium phenomena arising from infrequent collisions of gas particles by rarefied gas dynamics [28]. The shapes

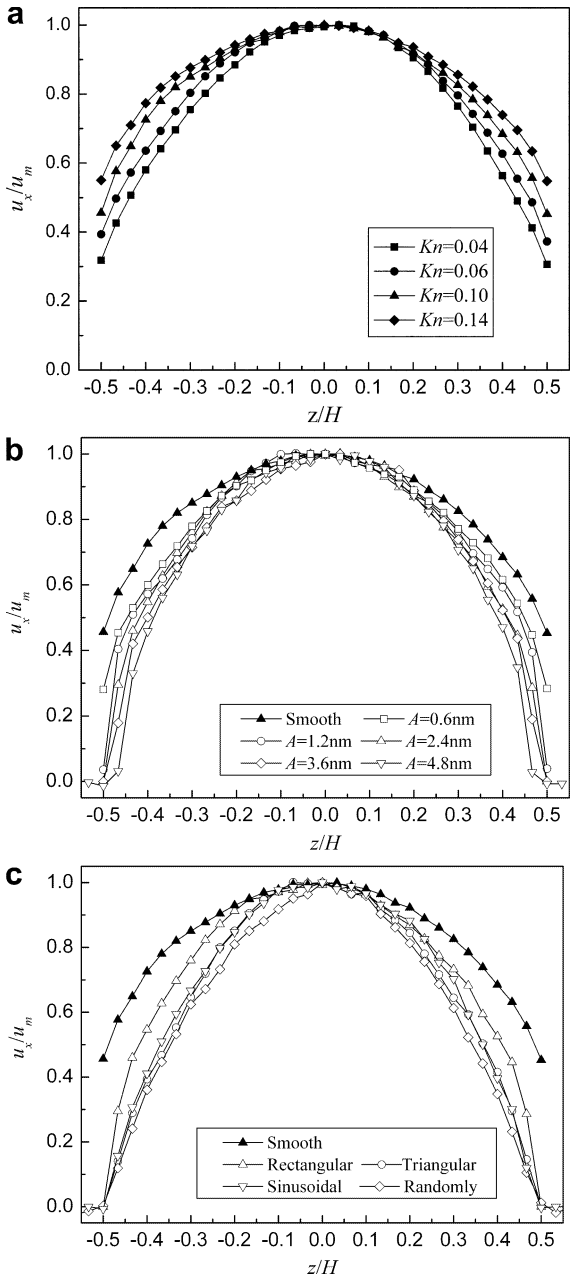

Fig. 2. Velocity profiles across the microchannel affected by the rarefaction and the surface roughness. (a) For smooth microchannels; (b) for microchannels with rectangular wave roughness ($Kn = 0.10$); (c) effect of the roughness geometry ($Kn = 0.10$, $A = 2.4$ nm).

of the profile curves at different Knudsen numbers are not completely similar because the effective viscosity is a function of the Knudsen number for rarefied gases [29].

Taking the case of the rectangular wave wall, we present the effect of the roughness height on the velocity profiles in Fig. 2(b). In the mainstream regime, the velocity profiles move downwards as the roughness increases. It indicates that the mean velocity is decreased by the surface roughness. Clearly, the surface roughness results in the deduction of the boundary velocity slip. For $A = 0.6$ nm, there is an apparent slip velocity $u_s = 0.2\sigma/\tau$. For $A = 1.2$ nm and 2.4 nm, the averaging macroscopic velocities of the gases on the walls are about zero, which means that the gases beneath the roughness diastemata are patches of backwater. However, the velocity slip can still be observed over the roughness element top. For a larger roughness, e.g. $A = 3.6$ nm,

the velocity slip due to the rarefaction disappears, which may indicate that a no-slip is induced by the surface roughness. For $A = 4.8$ nm, the roughness geometry occupies from $z/h = -0.5$ (0.5) to -0.45 (0.45). In the simulations, though there is no macroscopic motion for gases at the bottom of the roughness apertures, the gases in the upside of the apertures flows. The slip velocity extracted from Eq. (5) becomes negative, which is often defined as a negative slip [17,30]. Therefore, due to the roughness effect, general boundary conditions may cover the traditional slip, the no-slip and the negative slip.

Fig. 2(c) shows the effect of the roughness geometry on the velocity profiles with $Kn = 0.10$ and $A = 2.4$ nm. Among the four types of walls, the mean velocity is the largest for the flow in the rectangularly roughened microchannels and the smallest for the randomly triangular roughness channels for given Knudsen number and roughness height. The sinusoidal roughness has nearly the same effect on the velocity profile as the triangular one. It should be noted that the maximum roughness height is about 5.6 nm for the randomly triangular roughness corresponding to the RMS roughness of 2.4 nm. It indicates that the roughness geometry also has a significant effect on the gas microflows.

3.2. Boundary conditions

According to the Navier boundary condition [31], the slip length can be obtained by extrapolating the velocity profiles from the position in the fluid to where the velocity would vanish. In our simulations, the slip length L_s can be calculated by

$$L_s = u_s \Big/ \left(\frac{du_s}{dz}\right)_{|z|=h}. \tag{6}$$

A positive slip length represents the rarefaction effect where the fluid velocity would vanish within the solid. That the slip length is zero corresponds to the no-slip condition. A negative slip length denotes that the fluid velocity vanishes within the fluid and that the channel is narrowed by the surface roughness. The dimensionless slip length l_s is defined as $l_s = L_s/H$. For the slip boundary condition, Maxwell theory predicts that the dimensionless slip length is related to the Knudsen number as

$$l_s^M = \frac{2-\varsigma}{\varsigma} Kn \tag{7}$$

in which ς is the tangential momentum accommodation coefficient (TMAC), Kn is the Knudsen number defined as the ratio of the molecular MFP and the system characteristic length. The Maxwell theory indicates that the dimensionless slip length is determined by the Knudsen number linearly and is always positive caused by the rarefaction effect.

Fig. 3 summarizes our results about the dependence of the dimensionless slip length on the Knudsen number and the four types of the surface roughness. For flows in the smooth microchannels, the dimensionless slip length is clearly proportional to the Knudsen number where no-slip takes place as the Knudsen number goes to zero, which is in good agreement with the theoretical prediction of the Maxwell model. The slope of the l_s–Kn curve by a least-square method gives the TMAC $\varsigma = 0.28$ of gaseous argon over the smooth platinum surface at 120 K [32], which deviates the empirical value $\varsigma = 1.0$ in engineering situations. The results indicate that the Maxwell slip theory validates for the rarefied gases flowing over smooth surfaces. However, the surface roughness may cause significant deviation of the dimensionless slip length from the Maxwell model depending on the roughness geometry and height. For a given Knudsen number, a larger roughness may result in a smaller dimensionless slip length. Therefore, the dimensionless slip length of gas flows in microchannels is determined not only by the Knudsen number but also by the surface roughness. For a given roughness size, the slip length may increase with the increasing Knudsen number. With larger Knudsen numbers, the rarefaction effect is more evident as the dimensionless slip length appears positive. The dimensionless slip length may become negative as the Knudsen number goes to zero by extrapolating the l_s–Kn curve for slip flow in rough microchannels, which indicates the invalidation of the Maxwell model. The roughness effect is indicated to be significant for gas microflows at small Knudsen numbers.

In Fig. 3, the effect of the roughness geometries on the dimensionless slip length is also illustrated. For the rectangular wave wall, the dimensionless slip length is greater than zero in most region of the diagram and

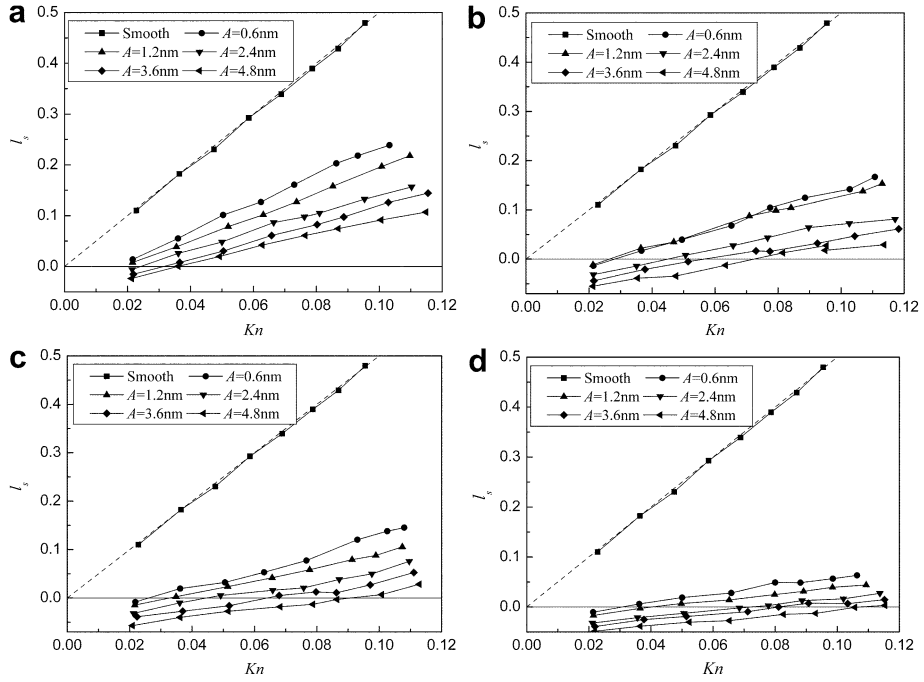

Fig. 3. Dimensionless slip length affected by the rarefaction and the surface roughness. The slip length of flows in smooth microchannels is presented in all the sub-figures for the eye guidance. (a) Rectangular wave roughness; (b) sinusoidal wave roughness; (c) triangular wave roughness; (d) randomly triangular wave roughness.

becomes negative at small Knudsen numbers and large surface roughness. For the other three types of roughness, the no-slip and negative slip may be caused by the surface roughness at moderate Knudsen numbers. For given Knudsen number and roughness height, the rectangular, sinusoidal, triangular and randomly triangular roughness respectively gives smaller dimensionless slip length in turn. In Mo's work [16], the ratio of the MFP and the roughness amplitude, λ/A, was suggested to replace the Knudsen number to validate the slip boundary conditions. However, our simulations indicate that the roughness size alone is probably not enough to represent the roughness effect considering the roughness geometry. In engineering situations of MEMS, the surface morphology should also be taken into account.

3.3. Friction coefficient

For the LFD laminar flows, the skin friction coefficient f is defined as

$$f = \frac{\tau_w}{\frac{1}{2}\rho u_0^2}, \tag{8}$$

where τ_w is the wall shear stress calculated by the net change of momentum of gas molecules at a wall per unit area and time in our simulations, ρ is the gas density and u_0 is the cross-sectionally averaged velocity. The product of the friction coefficient f and the Reynolds number Re is often referred to as the friction constant $C = fRe$. For the two-dimensional macroscopic flow, the Navier–Stokes equation is theoretically solved with the no-slip boundary condition to obtain the friction constant $C_0 = 96$. If the Maxwell slip law is considered, the normalized friction constant C^*, which represents the deviation degree of the friction coefficient from flows on the macroscale, can be theoretically expressed as [33]

$$C_t^* = \frac{C_t}{C_0} = \frac{1}{1 + 6\frac{2-\varsigma}{\varsigma}Kn}. \tag{9}$$

It indicates that the rarefaction effect always reduce the friction of slip flows.

Fig. 4 shows the friction constant obtained by our simulations as functions of the Knudsen number and the surface roughness. In the figures, the friction constant is normalized by $C_s^* = C_s/C_0$. For flows in the smooth microchannels, the effect of rarefaction on the normalized friction constant is presented in each figure. Clearly, the friction coefficient is reduced as the Knudsen number increases from 0.02 to 0.10. The trend of the decreasing friction constant with the increasing Knudsen number agrees with the theoretical prediction of Eq. (9) very well. The friction coefficient may be decreased by 42.4% at $Kn = 0.02$ and even by 78.7% at $Kn = 0.1$. It is also very clear that the deviation apparently emerges due to the surface roughness. As seen in Fig. 4, the normalized friction constant for flows in rough microchannels is larger than that in smooth microchannels and increases with the increasing roughness. The friction coefficient for flows in microchannels may be lower, equal, or higher than flows on the macroscale, which corresponds to the slip, no-slip, and negative slip boundary conditions. We can also find that the effects of the surface roughness and the rarefaction on the friction coefficient of slip microflows are strongly coupled. Under interactions of the Knudsen number and the surface roughness, the normalized friction constant may be changed by as high as +40% and as low as −60% for the Knudsen number ranging from 0.02 to 0.1.

In literatures, the increase of the friction coefficient by the presence of the surface roughness in microscale flows is often characterized by the relative roughness defined as A/H. It was shown that the roughness effect on the friction coefficient can be ignored with the relative roughness smaller than 5% [8]. In our simulations, the relative roughness ranges from 0.6% to 4.8%. Within the entire range of the relative roughness in our simulations, the roughness effect is significant. It may be partially due to the coupling of the rarefaction and the surface roughness.

Dependence of the normalized friction constant on the roughness geometries is also presented through comparing Fig. 4(a)–(d). It is shown that the roughness geometry has also an important effect on the friction coefficient. For given Knudsen number and roughness size, the randomly triangular type roughness channel presents a substantially higher friction coefficient than any other ones in the range of Knudsen numbers we studied.

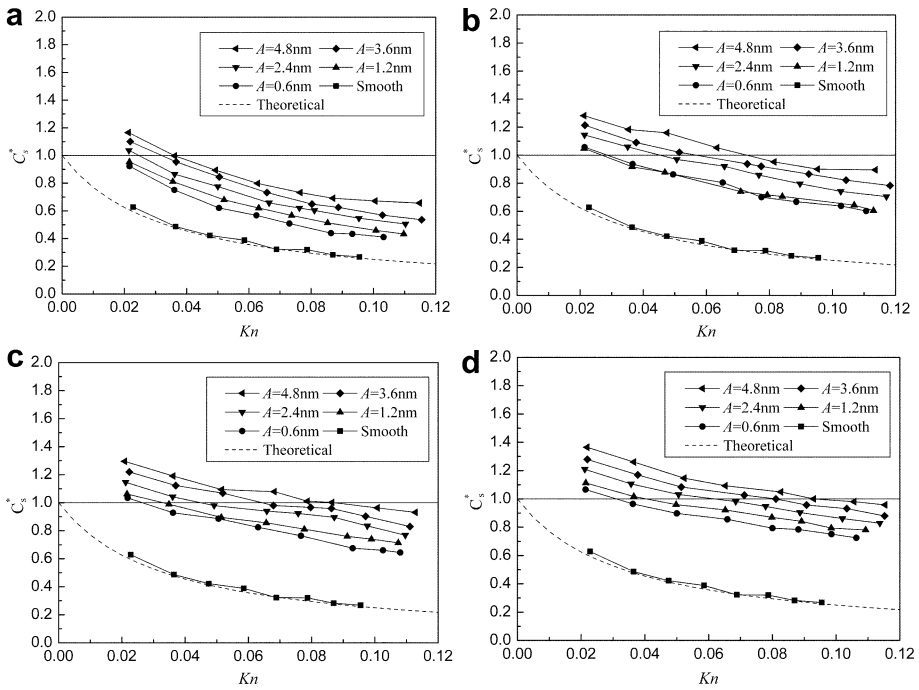

Fig. 4. Effects of the surface roughness and the Knudsen number on the normalized friction constant. (a) Rectangular wave roughness; (b) sinusoidal wave roughness; (c) triangular wave roughness; (d) randomly triangular wave roughness.

3.4. Streamlines near rough surfaces

Based on the continuum assumption, the microflow field in microchannels with uniformly distributed rough elements was analyzed by Du [8] and Hu et al. [9]. It was found that the roughness elements often caused the expansion and compression of the streamlines near rough surfaces, which was responsible to the increasing pressure drop of microflows. However, for rarefied gas flows in rough microchannels, the continuum models breakdown because of the rarefaction effect adjacent to surfaces. The molecule-based method is greatly needed.

The flow fields of gas microflows in rough channels are presented in Fig. 5. Fig. 5(a) and (b) consider the rectangular and the randomly triangular wave roughness respectively. In Fig. 5(a), we can find that the streamlines near the rough surfaces are clearly distorted. Over the rectangular roughness elements, the velocity slip can be observed evidently because the wall can be regarded to be smooth locally. Between every two elements, the streamlines are expanded, which implies the obstruction of the microflow by the roughness units directly. Beneath the most part of the diastemata between the roughness units, the gas has no macroscopic velocity along the flow direction. The flow recirculation found by the continuum method is not observed in our work. It may be due to the extreme diluteness of gases in the diastemata. Thus, beneath the diastemata are dead zones. In Fig. 5(b), similar characteristics can be observed that gases beneath the roughness diastemata are patches of backwater. The streamlines near the surfaces with the randomly triangular roughness are distorted

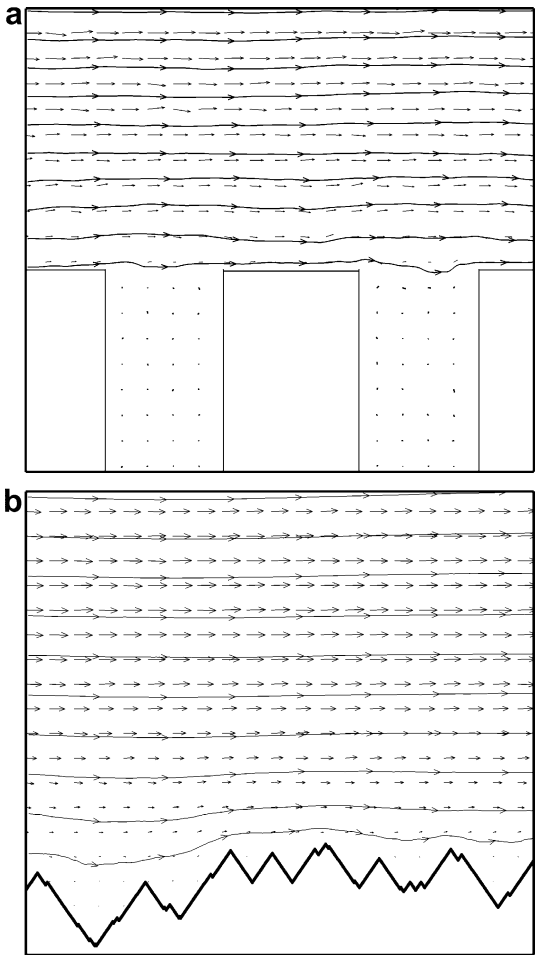

Fig. 5. Velocity field and streamlines of gas microflows near rough surfaces. (a) Rectangular wave roughness ($A = 4.8$ nm); (b) randomly triangular wave roughness ($A = 4.8$ nm).

more strongly than those with the rectangular roughness, which can unpuzzle that the friction coefficient of flows in randomly triangular roughness channels is larger than in rectangular ones.

In rarefied gas dynamics, the Maxwell model of the interaction of gas molecules and a wall is primarily based on the assumption of the bounce-back behavior, which is a linear combination of diffusive and specular reflections. This assumption may validate for mathematically smooth walls as shown by the above simulation results. However, from our MD simulation view, the backwater gases beneath the roughness diastemata may play an important role in the momentum exchange between gases and surfaces, because the molecules impinging the backwater may undergo many collisions in the roughness diastemata. It also indicates that the normal bounce-back assumption breakdowns. That means the gas molecules can penetrate through the wall boundary region occupied by the roughness diastemata, which is quite different from an imaginary mathematical surface. The roughness induced penetrability often reduces the velocity slip of rarefied gas flows.

Therefore, the surface roughness may affect the gas microflows in two ways: (a) the streamlines near surfaces are distorted; (b) the penetrability of surfaces is enhanced. For different geometries of the surface roughness, the distortion and the surface penetrability are both different. For very small roughness compared with the MFP, the two effects can be ignored. Generally, the MFP of a normal gas is about tens of nanometer which is actually comparable to the surface roughness in micro-devices. The two effects may become significant factors influencing the gas microflows.

4. Conclusions

Slip flows of gaseous argon in submicron platinum channels with surface roughness are investigated by the molecular dynamics simulation. The roughness is respectively modeled as the triangular, rectangular, sinusoidal and randomly triangular structures. The following conclusions may be drawn from the present study:

1. Resulted from the surface roughness, the boundary conditions of gas microflows are different from the Maxwell model: (a) the slip length is smaller than Maxwell model's prediction; (b) the slip length shows a non-linear relationship with the Knudsen number. The boundary conditions, including the slip, the no-slip and the negative slip, are determined not only by the Knudsen number but also the surface roughness.
2. The friction coefficient of gas microflows in channels with surface roughness is higher than that in smooth channels. The friction coefficient increases not only as the Knudsen number decreases but also as the surface roughness increases. The effects of the roughness and the rarefaction on the friction coefficient of gas microflows are strongly coupled.
3. The roughness geometry affects the boundary conditions and the friction characteristics significantly. It indicates that the roughness height alone is not enough to represent the roughness effect. For the four types of surface roughness studied in the present paper, the roughness effect increases in turn by the rectangular, sinusoidal, triangular and randomly triangular waves.
4. The surface roughness may act on the gas microflows in two ways: (a) the streamlines near rough surfaces are distorted; (b) the penetrability of rough surfaces is strengthened. The momentum exchange between gases and rough surfaces is accomplished via molecular behaviors of penetrating through the roughness diastema region undergoing multi-collisions.

Acknowledgement

This work was supported by the National Natural Science Foundation of China under grant number 10372051.

References

[1] C.M. Ho, Y.C. Tai, Micro-electro-mechanical systems (MEMS) and fluid flows, Annu. Rev. Fluid Mech. 30 (1998) 579.
[2] H.G. Craighead, Nanoelectromechanical systems, Science 290 (2001) 1532.

[3] P. Gravesen, J. Branebjerg, O.S. Jensen, Microfluidics – a review, J. Micromech. Microeng. 3 (1993) 168.
[4] M. Gad-el-Hak, Review: flow physics in MEMS, Mec. Ind. 2 (2001) 313.
[5] Z.Y. Guo, Z.X. Li, Size effect on microscale single-phase flow and heat transfer, Int. J. Heat Mass Transfer 46 (2003) 149.
[6] A.A. Rostami, A.S. Mujumdar, N. Saniei, Flow and hear transfer for gas flowing in microchannels: a review, Heat Mass Transfer 38 (2002) 359.
[7] L.F. Moody, Friction factors for pipe flow, Trans. ASME 66 (1944) 671.
[8] D.X. Du, Effect of compressibility and roughness on flow and heat transfer characteristics in micro-tubes, Ph.D. Dissertation, Tsinghua University, Beijing, China, 2000.
[9] Y.D. Hu, C. Werner, D.Q. Li, Influence of three-dimensional roughness on pressure-driven flow through microchannels, ASME J. Fluid Eng. 125 (2003) 871.
[10] G.E. Karniadakis, A. Beskok, Micro Flows: Fundamentals and Simulation, Springer-Verlag, New York, 2002.
[11] L.M. Phinney, G. Lin, J. Wellman, A. Garcia, Surface roughness measurements of micromachined polycrystalline silicon films, J. Micromech. Microeng. 14 (2004) 927.
[12] D. Resnik, D. Vrtacnik, U. Aljancic, S. Amon, Effective roughness reduction of {100} and {311} planes in anisotropic etching of {100} silicon in 5% TMAH, J. Micromech. Microeng. 13 (2003) 26.
[13] S.E. Turner, L.C. Lam, M. Faghri, O.J. Gregory, Experimental investigation of gas flow in microchannels, ASME J. Heat Transfer 126 (2004) 753.
[14] W. Sugiyama, T. Sawada, M. Yabuki, Y. Chiba, Effects of surface roughness on gas flow conductance in channels estimated by conical roughness model, Appl. Surf. Sci. 169–170 (2001) 787.
[15] H.W. Sun, M. Faghri, Effect of surface roughness on nitrogen flow in a microchannel using the direct simulation Monte Carlo method, Num. Heat Transfer Part A 43 (2003) 1.
[16] G. Mo, F. Rosenberger, Molecular-dynamics simulation of flow in a two-dimensional channel with atomically rough walls, Phys. Rev. A 42 (1990) 4688.
[17] B.Y. Cao, M. Chen, Z.Y. Guo, Rarefied gas flow in rough microchannels by molecular dynamics simulation, Chin. Phys. Lett. 21 (2004) 1777.
[18] G.M. Mala, D.Q. Li, Flow characteristics of water in microtubes, Int. J. Heat Mass Transfer 20 (1999) 142.
[19] J.A. Tichy, A porous media model for thin film lubrication, ASME J. Tribol. 117 (1995) 16.
[20] W.L. Li, J.W. Lin, S.C. Lee, M.D. Chen, Effects of roughness on rarefied gas flow in long microtubes, J. Micromech. Microeng. 12 (2002) 149.
[21] B.Y. Cao, M. Chen, Z.Y. Guo, Application of 2DMD to gaseous microflows, Chin. Sci. Bull. 49 (2004) 1101.
[22] Y.P. Chen, P. Cheng, Fractal characterization of wall roughness on pressure drop in microchannels, Int. Commun. Heat Mass Transfer 30 (2003) 1.
[23] J.C. Arnault, A. Knoll, E. Smigiel, A. Corner, Roughness fractal approach of oxidized surfaces by AFM and diffuse X-ray reflectometry measurements, Appl. Surf. Sci. 171 (2001) 189.
[24] P. Yi, D. Poulikakos, J. Walther, G. Yadigaroglu, Molecular dynamics simulation of vaporization of an ultra-thin argon layer on a surface, Int J. Heat Mass Transfer 45 (2002) 2087.
[25] J.R. Hook, H.E. Hall, Solid State Physics, second ed., Wiley, Chichester, 1991.
[26] M.P. Allen, D.J. Tidesley, Computer Simulation of Liquids, Oxford University Press, New York, 1987.
[27] G.S. Grest, K. Kremer, Molecular dynamics simulation for polymers in the presence of a heat bath, Phys. Rev. A 33 (1986) 3628.
[28] S.A. Schaaf, P.L. Chambre, Flow of Rarefied Gases, Princeton University, New Jersey, 1961.
[29] D.K. Bhattacharya, G.C. Lie, Molecular-dynamics simulation of nonequilibrium heat and momentum transport in very dilute gases, Phys. Rev. Lett. 62 (1989) 897.
[30] I.V. Ponomarev, A.E. Meyerovich, Surface roughness and effective stick–slip motion, Phys. Rev. E 67 (2003) 026302.
[31] S. GoldsteinModern Developments in Fluid Dynamics, vol. 2, Dover, New York, 1965.
[32] B.Y. Cao, M. Chen, Z.Y. Guo, Temperature dependence of the tangential momentum accommodation coefficient for gases, Appl. Phys. Lett. 86 (2005) 091905.
[33] J.C. Harley, Y. Huang, H.H. Bau, J.N. Zemel, Gas flow in microchannels, J. Fluid Mech. 284 (1995) 257.